IEEE Access
Multidisciplinary ⋮ Rapid Review ⋮ Open Access Journal

Received November 17, 2019, accepted December 3, 2019, date of publication December 9, 2019, date of current version December 23, 2019.

Digital Object Identifier 10.1109/ACCESS.2019.2958496

Design of CRLH Leaky-Wave Antenna With Low Sidelobe Level

QINGSHAN YANG[1], (Member, IEEE), XIAOWEN ZHAO[1], (Member, IEEE), AND YUNHUA ZHANG[1,2], (Member, IEEE)

[1]CAS Key Laboratory of Microwave Remote Sensing, National Space Science Center, Chinese Academy of Sciences, Beijing 100190, China
[2]School of Electronic, Electrical and Communication Engineering, University of Chinese Academy of Sciences, Beijing 100049, China

Corresponding author: Qingshan Yang (flyangster@gmail.com)

This work was supported in part by the National Natural Science Foundation of China under Grant 61501432, and in part by the Youth Innovation Promotion Association of Chinese Academy of Sciences under Grant 2017189.

ABSTRACT Composite right/left-handed (CRLH) waveguide leaky-wave antenna (LWA) with low sidelobe level (SLL) and high radiation efficiency is investigated and designed in this paper. Due to the characteristic of negative and positive dominant mode propagation constant of the CRLH transmission line, a backward to forward beam-steering LWA can be realized through frequency scanning. The leaky-wave radiation is analyzed first based on a Ka-band CRLH waveguide with straight slots differently offset on the broadwall. The propagation constant maintains almost invariable as the slot offset varies, meanwhile the attenuation constant has a considerable dynamic range. Thus meandering long slot, whose offset varies along the CRLH waveguide, can be cut on the broadwall to generate a tapered excitation distribution. A prototype of the proposed CRLH waveguide LWA with meandering long slot is designed and fabricated to validate the design. Measurement results show that continuous beam-steering capability from −29° to +31° is achieved, meanwhile the optimized SLLs for the designed antenna patterns are kept below −**18.5** dB in the major operating band with the minimum SLL of −**22.4** dB at 33 GHz, and the average radiation efficiency is 65.4%. The realized SLLs and radiation efficiency performances of our CRLH LWA surpass others reported in open literatures.

INDEX TERMS Beam-steering, composite right/left-handed (CRLH), leaky-wave antenna, meandering long slot, sidelobe level (SLL), tapered distribution.

I. INTRODUCTION

Beam-steering capability is highly demanded in many radars systems, especially in tracking radars. Compared with mechanically scanned arrays, electronically scanned ones are more preferred in practical radar systems because of their fast beam switching capability. Frequency scanning and phase scanning are two general approaches for electronic beam-steering. Phased arrays have been applied widely for their continuous beam scanning capability from backfire to endfire, however, the feed network is often complicated and the cost is high because large amount of Tx/Rx modules are used. Frequency scanning antennas (FSAs) can have low cost without using Tx/Rx modules. There are generally two types of antennas for traditional FSAs. One type of FSAs is leaky-wave antennas (LWAs), which usually support one or several leaky waves [1]. For uniform LWAs, the feed structures are simple, however, the beam can only scan in the forward directions since the propagation constant is always positive. For the periodic LWAs, backward radiation can be achieved by using a negative space harmonic in addition to forward radiation using a positive space harmonic. However, broadside radiation is not possible for either type of traditional LWAs. Another type of FSAs is composed of linear antenna array series fed by sinuous feed system [2], which can radiate from backfire to endfire through frequency scanning. Rectangular waveguide operating in the dominant mode is often used for the feed systems due to its high power capacity, low loss as well as high dispersion which enhances the scan sensitivity. However, since a sinuous feed has a large number of 180° bends, the design of the bends is quite critical for the impedance match, otherwise, a large input VSWR will occur at the broadside-beam position frequencies. In addition, both forward and reverse directional couplers are needed to

The associate editor coordinating the review of this manuscript and approving it for publication was Mohammad Zia Ur Rahman.

This work is licensed under a Creative Commons Attribution 4.0 License. For more information, see http://creativecommons.org/licenses/by/4.0/

excite the radiating elements, which make the structure quite complicated.

Composite right/left-handed (CRLH) metamaterials have been a research hotspot over the past decades due to their unique properties such as backward wave and infinite wavelength propagation, which can be applied to LWAs to realize continuous beam-steering from backfire to endfire [3]. Many CRLH LWAs have been proposed with similar design procedures so far using planar transmission line structures and waveguide structures [4]–[9]. A balanced CRLH unit cell is first optimized to ensure a continuous beam-steering from backward to forward directions including the broadside direction. Then the LWA is simply constructed by periodically cascading the CRLH radiating unit cells. Exponential attenuation distribution is formed along the LWA aperture since all the unit cells are the same, which will lead to high sidelobe level (SLL) in the radiation patterns.

In recent years, several researches have been done trying to reduce the SLL and improve the performance of the CRLH LWAs. We have proposed a CRLH ridge substrate integrated waveguide (RSIW) slot array antenna in [10]. Longitudinal slots with varied offsets were adopted on the surface of the CRLH RSIW to achieve a tapered excitation distribution. The SLLs of this slot array antenna radiation patterns are below -15 dB in the left-handed (LH) region. The SLLs in the right-handed (RH) region, however, are only about -10 dB, which still need to be improved. In [11] and [12], tapered CRLH LWAs are studied to optimize the SLL of the antenna patterns, they were both realized by using non-uniform CRLH unit cells, the attenuation constants of the unit cells were controlled by the gap of the interdigital capacitor. Nevertheless, the SLLs for both LWAs were optimized only at one single frequency. A CRLH substrate integrated waveguide (SIW) LWA with low SLL was designed in [13], this work provided a sparse array design using identical interdigital capacitor to realize a tapered excitation distribution. Only simulated results showed that -15 dB SLLs were achieved in a narrow beam-steering range from $-3.6°$ to $+7.6°$. Recently, researches on the periodic LWAs have been carried out with the open-stopband (OSB) suppressed to achieve continuous beam-steering capability [14]–[16]. The -1 space harmonic is used to radiate and the OSB were eliminated by introducing another perturbation (a nonidentical transverse slot [14], shorting vias [15], or longitudinal slot [16]) to eliminate the series inductance of a transverse slot on the SIW. However, the tapered excitation distribution of the LWAs for low SLL was also not reported.

The waveguide type CRLH LWAs are better choices than the planar ones for practical radar systems because of their capability of handling higher power than the planar ones. A CRLH rectangular waveguide with dielectric-filled corrugations was originally proposed in [17] and applied to LWA in [18], [19]. However, the dielectric-filled corrugations brought so large dielectric losses that the LWA suffers from low radiation efficiency. A transverse slot array using an air-filled CRLH waveguide was proposed in [20], where the radiating slot is confined to the CRLH unit cell. Although the dielectric loss is avoidable, the antenna is constructed directly by cascading the radiating CRLH unit cells as the planar CRLH LWAs are, so it does not have a tapered excitation distribution for low SLL of the radiation patterns.

CRLH waveguide with air-filled double ridge corrugations (DRCs) was first proposed and the LH propagation was investigated using full-wave simulation in [21]. This CRLH waveguide has the advantages of high power capacity, low loss and relative easy to fabricate, and will be a good choice in practical radar applications. We will exploit this CRLH waveguide to design a high performance CRLH LWA with low SLL and high radiation efficiency. The previous related studies can be found in [22]–[25]. This paper is organized as follows. Section II gives a parametric study of the CRLH unit cell to show a general method of design this type of CRLH structure. The dispersion characteristics of the leaky-wave radiation using full-wave simulation are also analyzed in this section including the propagation constant and attenuation constant. The design procedure of high performance CRLH LWA is given in Section III. Section IV shows the simulated and measured results and discusses the performance of the proposed antenna. Finally, conclusion is drawn in Section V.

II. DISPERSION ANALYSIS

Fig. 1 depicts the configurations of the air-filled CRLH waveguide unit cell adopted in this paper. It is composed of a traditional rectangular waveguide with its one broadwall

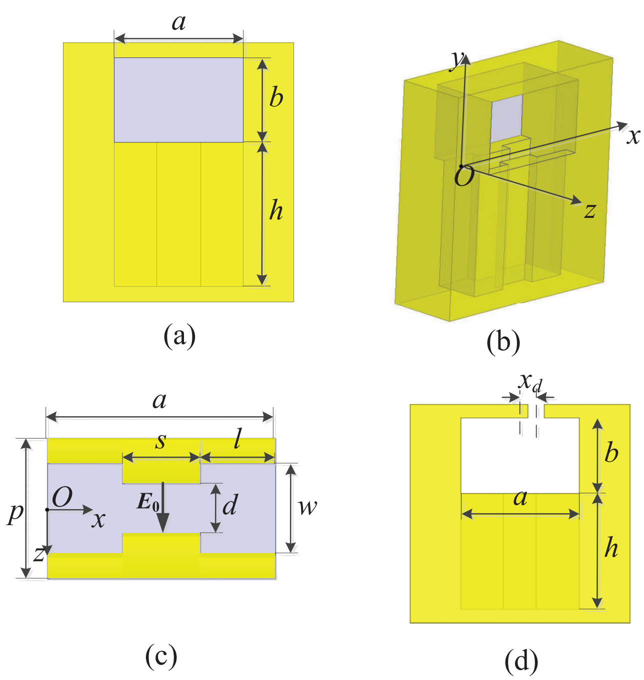

FIGURE 1. Configuration of the Ka-band CRLH waveguide unit cell. (a) Side view of the closed unit cell (b) 3-D view of the closed unit cell (c) Top view of the unit cell (d) radiating unit cell with longitudinal slot. The optimized geometric parameters are: $a = 4.37$ mm, $b = 2.8$ mm, $h = 4.33$ mm, $d = 1$ mm, $l = 1.585$ mm, $p = 2.8$ mm, $s = 1.2$ mm, $w = 1.8$ mm.

periodically loaded with air-filled short-circuited DRCs. The unit cell configuration of this CRLH waveguide is depicted in Fig. 1 (a)-(c). A CRLH waveguide can be constructed by periodically cascading the unit cells. The RH propagation, i.e. the forward wave propagation is supported by the dominant mode of the main rectangular waveguide above its cutoff frequency. While below the cutoff frequency, an inherent shunt inductance exists for the main waveguide, the loaded short-circuited DRCs will provide a series capacitance for the main waveguide below the cutoff frequency, thus the LH propagation, i.e. the backward wave propagation is generated. This means that the CRLH waveguide is operating in the dominant mode supporting both the backward wave and forward wave propagation simultaneously. Stepped transitions can be introduced in the two ends of the CRLH waveguide for connecting the structure to standard waveguides.

Concluded by our previous work in [25], the surface current distribution is very similar to that of the traditional rectangular waveguide. Only x component exists at the two sides of the broadwall ($x = 0$ and $x = a$) with equal amplitude but opposite direction. While only z component appears at the centerline ($x = a/2$), no radiation would occur for the longitudinal slot situated along the centerline of the broadwall because the surface current is not cut. However, the power can be leaked from the longitudinal slot cut on the broadwall with offsets from the centerline since the x components of the surface current can be cut. Besides, the bigger slot offset leads to the larger attenuation constant. A radiating unit cell is shown in Fig. 1 (d). The comparison of the full-wave simulation for the surface current of this CRLH waveguide with the analytical derivation is performed in the previous work in [25]. This characteristic is the principle for designing high performance CRLH LWAs because the slot offsets can be varied to realize a tapered excitation distribution to achieve low SLL of radiation patterns.

As shown in Fig. 1 (d), a straight slot with offset x_d is cut on the smooth broadwall. A balanced case of the CRLH structure should be optimized since broadside radiation is concerned in this work. The slot width w_{slot} is chosen to be 0.6 mm, which is far less than the wavelength in the free space. In this section, full-wave simulation using Ansoft's High Frequency Structure Simulator (HFSS) is performed based on the Ka-band CRLH waveguide.

A. PARAMETRIC STUDY FOR THE CRLH LWA UNIT CELL

Dispersion is the key parameter to design a CRLH structure because LH region, RH region and the stop band (or transition frequency) can be distinguished clearly from the dispersion curve. As is known to all, the dispersion of the CRLH structure is sensitive to gemometric parameters. The effect of various parameters to the CRLH characteristic is first studied to give a guidance to the balanced CRLH LWA unit cell design.

As stated above, this CRLH waveguide is operating in the dominant mode, thus the cutoff frequency of the main waveguide, which is also the transition frequency or the stop-band region for the CRLH waveguide, is mainly determined by the main waveguide width a. Fig. 2 shows the effect of the main waveguide width a on the propagation constant β. It is observed that the transition frequency of the CRLH unit cell is decreasing as the main waveguide width a is increasing. Bandgap appears when a increases at a certain value since the operating frequency of required capatively loaded DRC is far lower than the cutoff frequency of the main waveguide.

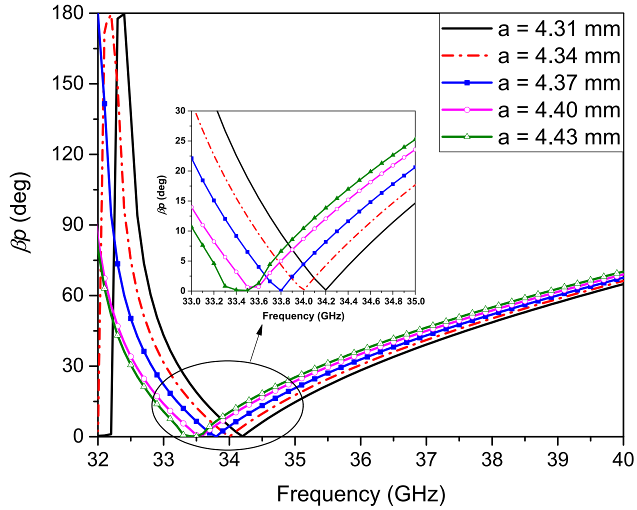

FIGURE 2. **Propagation constant β versus the main waveguide width a. The other parameters are: $b = 2.8$ mm, $h = 4.33$ mm, $d = 1$ mm, $l = 1.585$ mm, $p = 2.8$ mm, $s = 1.2$ mm, $w = 1.8$ mm.**

The depth of the DRC h mainly affects the series capacitance for the CRLH unit cell, thereby the series resonant frequency for the LH propagation. As the value of h changes, the corresponding propagation constant β is depicted in Fig. 3. As can be seen, the series resonance is

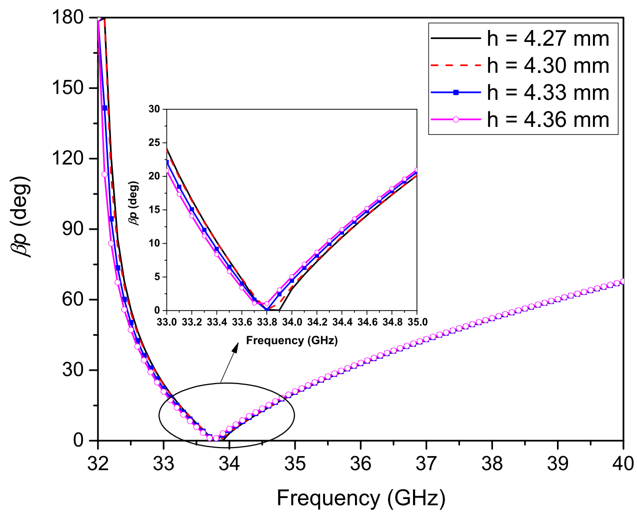

FIGURE 3. **Propagation constant β versus the DRC depth h. The other parameters are: $a = 4.37$ mm, $b = 2.8$ mm, $d = 1$ mm, $l = 1.585$ mm, $p = 2.8$ mm, $s = 1.2$ mm, $w = 1.8$ mm.**

moving towards to the lower frequencies when the depth of the DRC increases, which is because of the increase value of the series capacitance; while the cutoff frequency of the main waveguide nearly changes, which locates at 33.8 GHz.

The effects of the DRC parameters s and w on the propagation constant are given in Fig. 4 and Fig. 5, respectively. As clearly shown, the operating frequency of the DRC decreases as the parameters s and w increase. The cutoff frequency of the main waveguide is unchanged since it is mainly determined by the waveguide width a. The final optimized geometric parameters are given in the caption of Fig. 1.

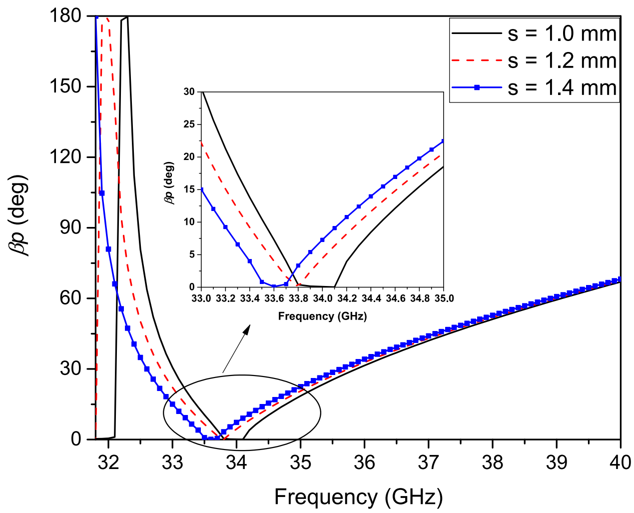

FIGURE 4. **Propagation constant β versus s. The other parameters are: $a = 4.37$ mm, $b = 2.8$ mm, $h = 4.33$ mm, $d = 1$ mm, $l = 1.585$ mm, $p = 2.8$ mm, $w = 1.8$ mm.**

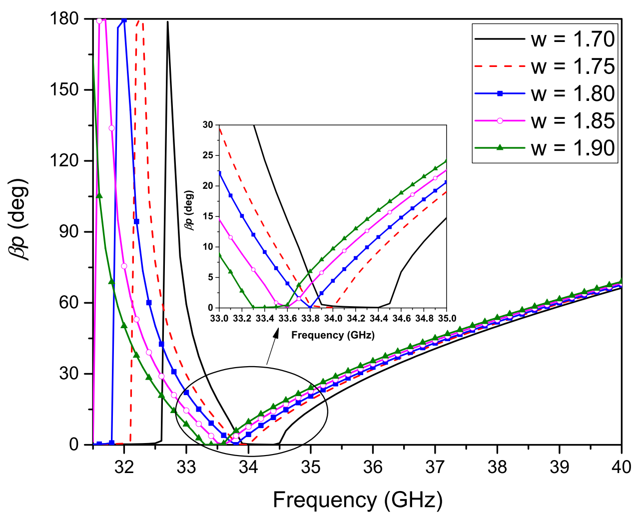

FIGURE 5. **Propagation constant β versus w. The other parameters are: $a = 4.37$ mm, $b = 2.8$ mm, $h = 4.33$ mm, $d = 1$ mm, $l = 1.585$ mm, $p = 2.8$ mm, $s = 1.2$ mm.**

Learned from the parametric study, one can see that the RH propagation starts from the cutoff frequency of the main waveguide, which is determined by the waveguide width a. The LH propagation is affected by the parameters of the DRC. Balance condition for the CRLH unit cell can be achieved by optimizing the different parameters responsible for the LH and RH propagation, respectively. Thus this design can be treated as a general technique to obtain similar CRLH structures for different operating frequencies.

B. PROPAGATION CONSTANT β VERSUS SLOT OFFSET

HFSS eigenmode solution with periodic boundary is adopted in the simulation of propagation constant β versus slot offset, which is believed to be more accurate compared with the driven modal simulation based on S-parameters when calculating the propagation constant [6]. In a general procedure of designing a CRLH structure, the driven modal analysis based on S-parameters is firstly used for fast calculation, and then the optimized structure is validated by the more accurate but time-consuming eigenmode solution. This is because the propagation phase behavior in the periodic structure is concerned, thus the model with periodic boundary condition is more accurate than the driven modal analysis based on S-parameters of truncated structure with only finite unit cells. The slot offset x_d is varied at every 0.1 mm from 0.1 mm to 0.9 mm. A group of propagation constant curves is obtained and plotted in Fig. 6. It is observed that the transition frequency of the designed Ka-band CRLH LWA unit cells is about 33.8 GHz. Small bandgaps nearby the transition frequency appears in the dispersion curves when the slot offsets become bigger. This should be ascribed to the fact that the CRLH structures are very sensitive to geometric size, the balance condition would be deteriorated when the slot offset varies. In our previous simulation in [23], when the slot offset changes, the geometric parameters of the DRC, e.g. the depth h, can be adjusted accordingly to maintain the CRLH unit cell balanced. However, this operation would increase the manufacturing difficulty. Thus in this work, the parameters of the DRCs are constant for all the CRLH unit cells. Although the deterioration of the dispersion is unavoidable, it is acceptable in practical designs since the bigger slot offsets are not frequently used in the design of tapered excitation distribution. A tradeoff between the antenna performance and fabrication is made in the choice of DRCs' depth. It is clearly seen from Fig. 6 that the propagation constant β only changes slightly as the slot offset varies from 0.1 mm to 0.9 mm, which guarantees the requirement of the propagation constant in the design a tapered LWA.

C. ATTENUATION CONSTANT α VERSUS SLOT OFFSET

The attenuation constant α can be calculated by building a CRLH prototype with 5 unit cells shown in Fig. 1 (d). The conductor material is set to be perfect electric conductor (PEC), thus the leaky-wave radiation is the only reason for the loss. In the simulation, the slot offset is varied at every 0.01 mm from 0.01 mm to 0.9 mm. Fig. 7 shows the simulated attenuation constant α versus the slot offset x_d at the transition frequency of 33.8 GHz. For the convenience of design procedure, the relationship between the attenuation constant

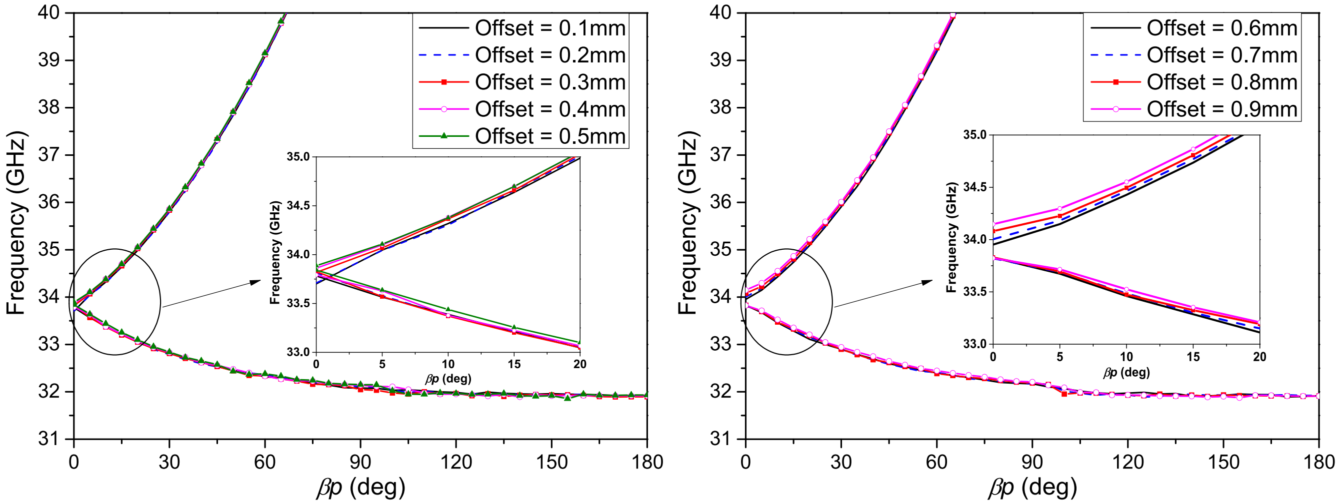

(a) (b)

FIGURE 6. Propagation constant curves of the Ka-band CRLH LWA. (a) Slot offset from 0.1 mm to 0.5 mm (b) Slot offset from 0.6 mm to 0.9 mm.

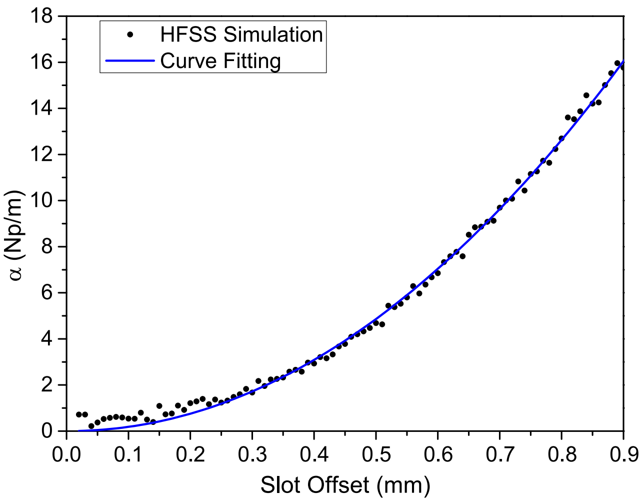

FIGURE 7. Attenuation constant α versus the slot offset x_d at the transition frequency of 33.8 GHz.

and the slot offset can be expressed in analytical form using curve fitting technique. Considering that no radiation occurs when slot offset is zero, a power function model can be applied as

$$\alpha = Ax_d^B \tag{1}$$

where $A = 19.88$, $B = 2.032$, and the R-square is 0.9974 and root mean square error (RMSE) is 0.305. The fitting curve is also plotted in Fig. 7 for comparison. As clearly shown, the fitness can be satisfied, a considerable dynamic range of 16 Np/m for the attenuation constant α changes as the slot offset x_d varies by 0.9 mm. According to the propagation constant β in Fig. 6, the slot offset value more than 0.6 mm leads to a slight unbalanced state of the CRLH LWA structure. It should be noted that the propagation constant is calculated based on periodic boundary with infinite unit cells. While the attenuation constant is calculated based on the S-parameters of a CRLH prototype with 5 unit cells. Besides, the transition frequency of 33.8 GHz locates at the edge of the bandgap, so the attenuation constant α still has a smooth variation in Fig. 7. The behavior of attenuation constant α versus frequency is also analyzed using 5 unit cells and given in Fig. 8. It is observed that the stopband is mitigated when the slot offset is getting smaller. This is in accordance with the behavior of propagation constant in Fig. 6 that the balance condition of the CRLH waveguide is deteriorated when the slot offset is getting bigger. We should point out that the deterioration of the balance condition is not the main reason for the bump of attenuation constant in Fig. 8. It is observed from Fig. 8 that the bump corresponds to the frequency region nearby the transition frequency (i.e. the cutoff frequency of the main

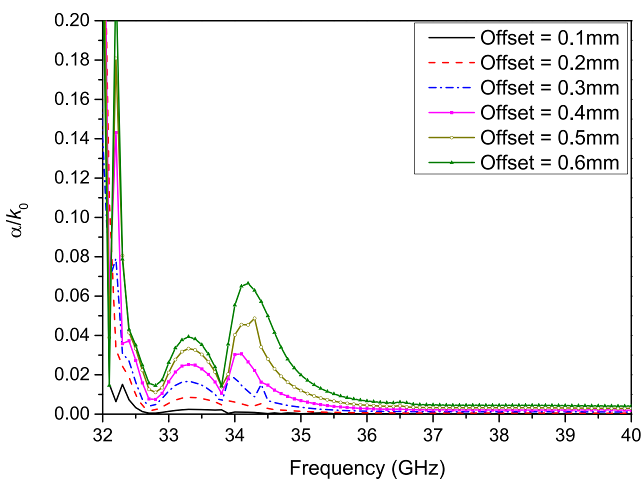

FIGURE 8. Normalized attenuation constant of the CRLH structure versus frequency with different slot offset.

waveguide), not the stopband (small gap between 33.8 GHz and 33.9 GHz). The bump is mainly due to that the LH region of CRLH structure locates below the cutoff frequency of the main waveguide, thus the attenuation constant nearby the cutoff frequency is larger. Similar phenomenon can be found in a planar CRLH LWA in [7]. This is very different from the periodic LWAs where the bump of the attenuation constant corresponds exactly to the OSB of the propagation constant [14], [15].

III. DESIGN PROCEDURE OF CRLH LWA

The design procedure of the high performance CRLH LWA takes the classic method for a traditional uniform LWA [1]. In order to achieve high gain and efficiency, a long effective aperture and small attenuation constant are required. A CRLH waveguide composed of 100 unit cells is used to design the LWA, and the desired pattern for this antenna is specified as a Taylor radiation pattern with −30 dB SLL.

A. RELATION BETWEEN LEAKY-WAVE FACTOR AND ELEMENT POSITION

For simplicity, the LWA based on the 100-unit-cell CRLH waveguide is first discretized as a 50-element array, which means the element distance is the length of 2 unit cells. The normalized excitation amplitudes $A(n)$ can be calculated using standard antenna synthesis techniques, where the element number n is labeled from the feeding side of the CRLH waveguide.

The corresponding attenuation constant α is then determined by [1]

$$2\alpha(n) = \frac{|A(n)|^2}{\frac{1}{\eta}\sum_{i=1}^{50}|A(i)|^2 - \sum_{i=1}^{n}|A(i)|^2} \tag{2}$$

where η is the radiation efficiency. Usually 100% radiation efficiency is not allowed since it would lead to very large attenuation constant in the end of the LWA, thus $\eta = 0.95$ is used in our design. It should be pointed out that the antenna length and the efficiency is carefully chosen to make the required attenuation constants along the antenna in a relative low level in order to achieve a high gain. Besides, lower attenuation constant corresponds to better behavior of the dispersion as analyzed above. The relation between the attenuation constant α and the element number (actually the element position) is calculated using (2) and plotted in Fig. 9.

B. RELATION BETWEEN SLOT OFFSET AND ELEMENT POSITION

The relation of the attenuation constant α and the slot offset x_d has been established in (1), together with (2), the relation between the slot offset and the element number can be determined. Fig. 9 also gives the slot offsets corresponding to the element number. In this way, the tapered geometry of the designed CRLH LWA is achieved.

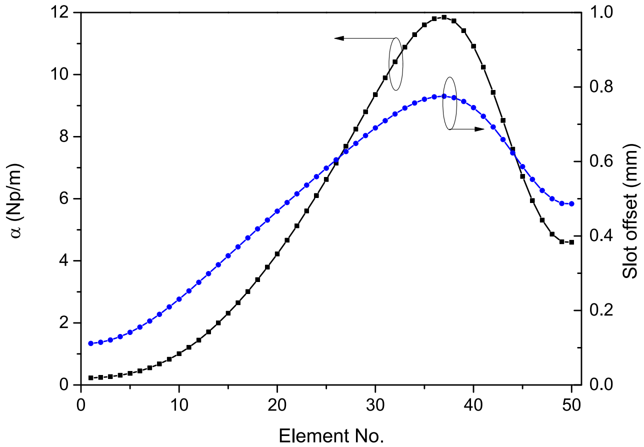

FIGURE 9. Attenuation constant α and slot offset versus element position at the transition frequency of 33.8 GHz.

IV. CRLH WAVEGUIDE LWA WITH LOW SLL

Aluminum alloy is used and sandwiched structure is adopted in the fabrication process, as shown in Fig. 10, the air-filled DRCs is sandwiched between the bottom metal wall and the top slotted metal wall. Stepped transitions are applied in the two ends to match the CRLH waveguide to the standard WR-28 waveguide. The coordinate axes are rearranged for expressing the radiation patterns conveniently. The CRLH waveguide LWAs is simulated using CST Microwave Studio and measured by Aglient PNA-X vector network analyzer.

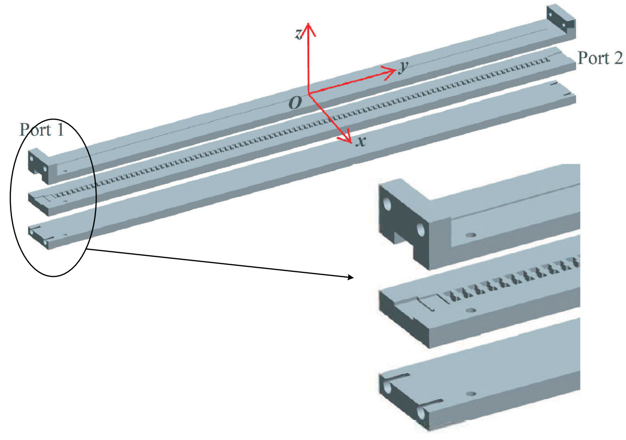

FIGURE 10. Sandwiched structures of the proposed CRLH waveguide LWA in the fabrication process.

Fig. 11 presents the simulated and measured S-parameters of the synthesized meandering long slot CRLH waveguide LWA. The measurement is calibrated on the waveguide port of the LWA with the effect of the coaxial-to-waveguide transducer excluded. The amplitude difference between the simulated and measured S_{21} mainly attributes to that the aluminum alloy is actually used in the fabrication, and its conductivity is lower than that of pure aluminum, thus the conductor loss of the fabricated prototype is larger than that of the simulated prototype. In addition, the roughness of

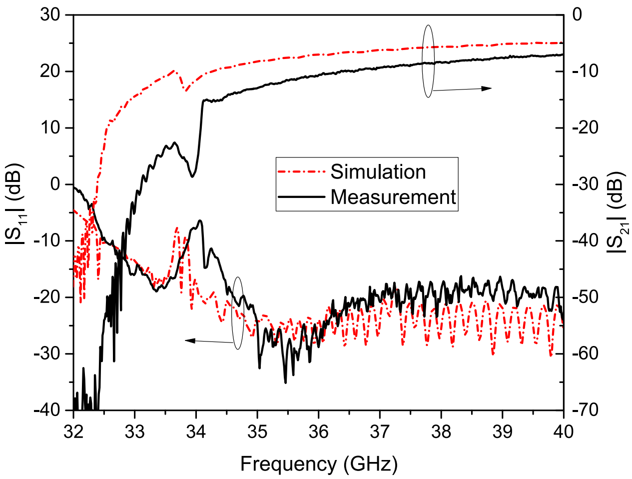

FIGURE 11. Simulated and measured *S*-parameters of the meandering long slot CRLH waveguide LWA.

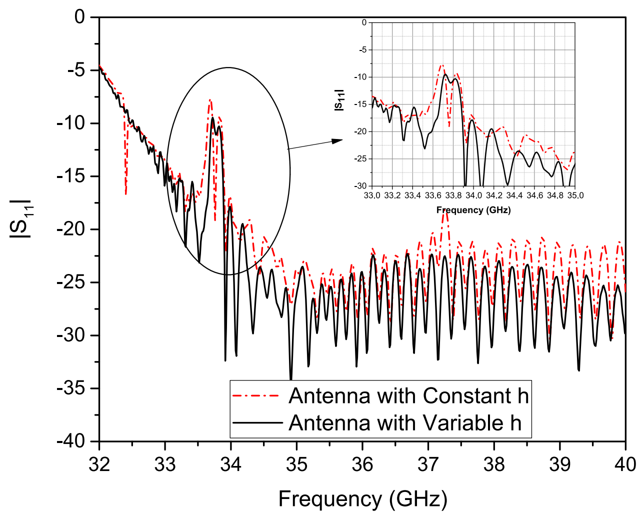

FIGURE 12. Simulated $|S_{11}|$ of the CRLH LWAs with constant and variable *h*.

the actual aluminum alloy is not considered in the simulation. The simulated S_{11} nearby the transition frequency of 33.8 GHz is a little higher than -10 dB, which is believed to blame the deterioration of the CRLH balance condition. If the depth of the DRC h is varied accordingly when the slot offset is changed, a better balance condition and reflection loss can be achieved, as shown in Fig. 12. The measured S_{11} plotted in Fig. 11 is in accordance with the simulated result except a little increase of the reflection loss nearby the transition frequency. It is a little difficult to optimize since a large number of unit cells (100 unit cells) is adopted in our design, the accumulated fabrication error will increase the optimization difficulty. Matching dowels can be adopted to improve the matching problem in the measurement. In order to evaluate the performance of the LWA radiation affected by the deterioration of the balance condition, loss analysis for this CRLH LWA is investigated using (3).

$$Loss = 1 - S_{11} \cdot S_{11}^{*} - S_{21} \cdot S_{21}^{*} \tag{3}$$

Both the simulated and measured loss are calculated and given in Fig. 13, from which one can see that the measured loss including the conductor loss and radiation is higher than the simulated one in most operating frequency region. This is in accordance with the analysis of S_{21} magnitude stated above. However, the measured loss is lower than the simulated one nearby the transition frequency, which is due to the increased measured return loss caused by the manufacture error compared with the simulated one shown in Fig. 11. Despite that, above 70% power is radiated and dissipated observed from the measured loss.

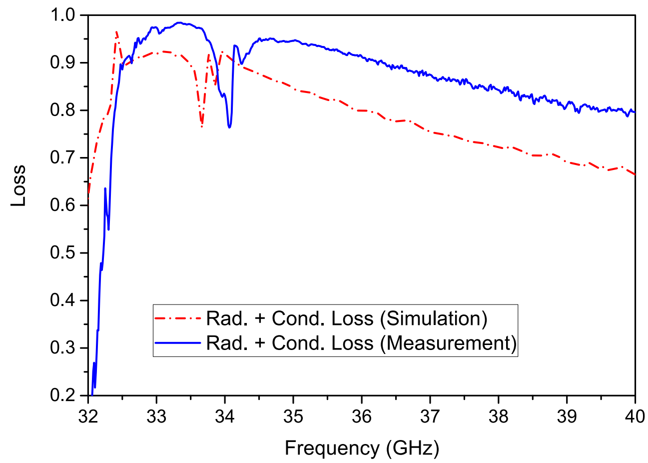

FIGURE 13. Simulated and measured losses of the meandering long slot CRLH waveguide LWA.

The radiation patterns of this meandering long slot CRLH waveguide LWA are measured using near-field antenna measurement system, as shown in Fig. 14. Fig. 15 gives the simulated and measured normalized radiation patterns in the

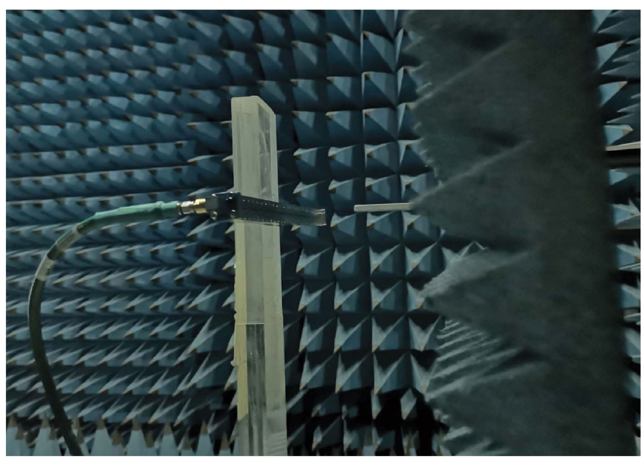

FIGURE 14. Meandering long slot CRLH waveguide LWA measurement in the near-filed chamber.

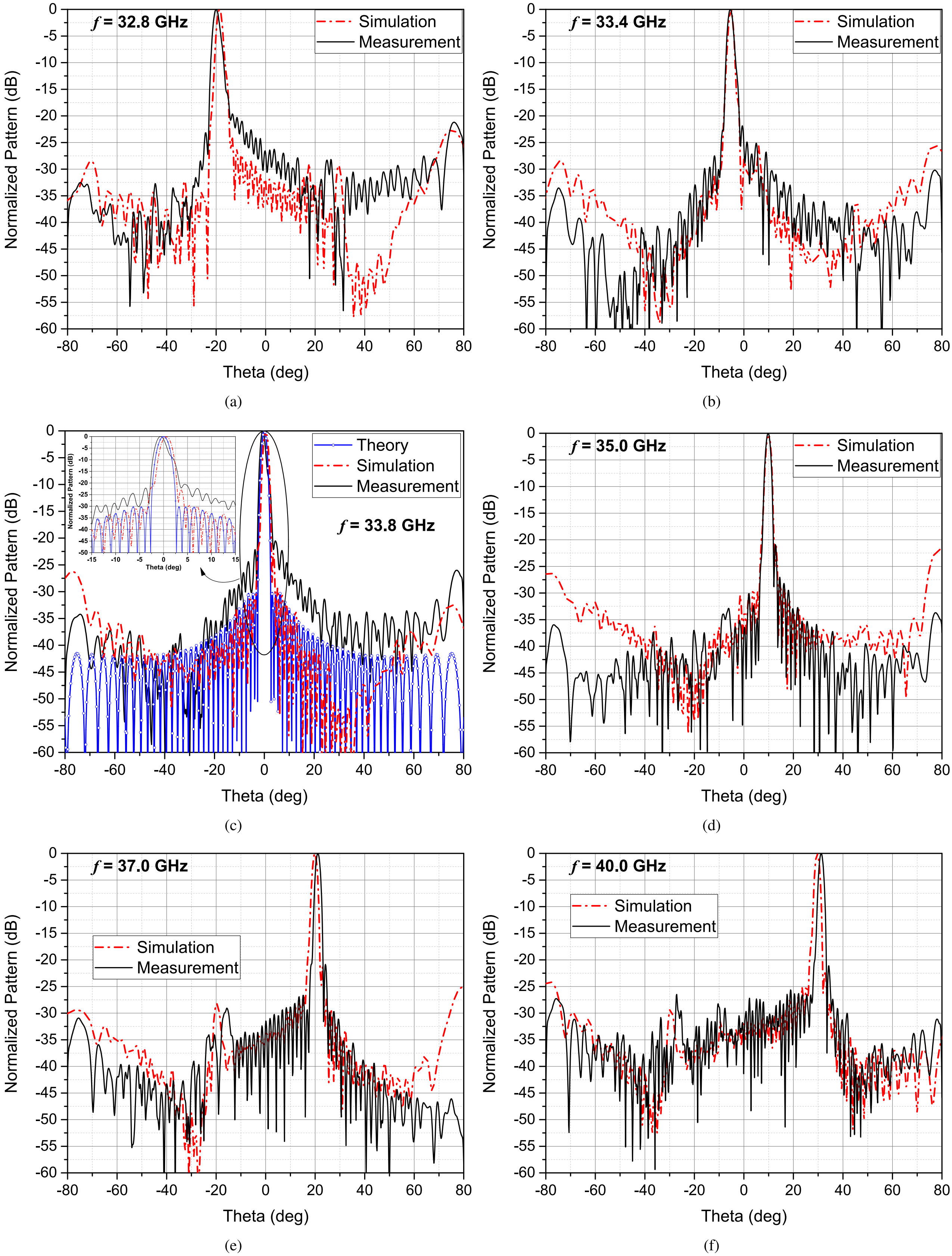

FIGURE 15. Simulated and measured normalized radiation patterns for (a) 32.8 GHz, (b) 33.4 GHz, (c) 33.8 GHz, (d) 35.0 GHz, (e) 37.0 GHz, (f) 40.0 GHz.

y-z plane. A good agreement can be observed. A cross-polarization level below −50 dB is achieved, which can be negligible. In the broadside pattern of Fig. 15(c), the theoretical Taylor pattern is also plotted for comparison. The simulated and measured sidelobe level ratio (SLR) is about 23 dB and 21 dB, respectively. The target SLR of 30 dB is not precisely met, which can be attributed to the inaccuracy between the discrete linear sources and the continuous ones, as well as the internal high-mode coupling that has not been considered in the design procedure. A potential method that reduces the SLR difference between the simulated patterns and the theoretical ones would be using the continuous linear source instead of the discrete one, and calculate the tapered geometry using analytical expression. The measured mainlobe directions and SLRs of the designed CRLH LWA are plotted in Fig. 16. Beam-steering range from −29° to +31° including the broadside direction is realized when the frequency scans from 32.6 GHz to 40 GHz. The SLRs above 18.5 dB are achieved in the major operating band.

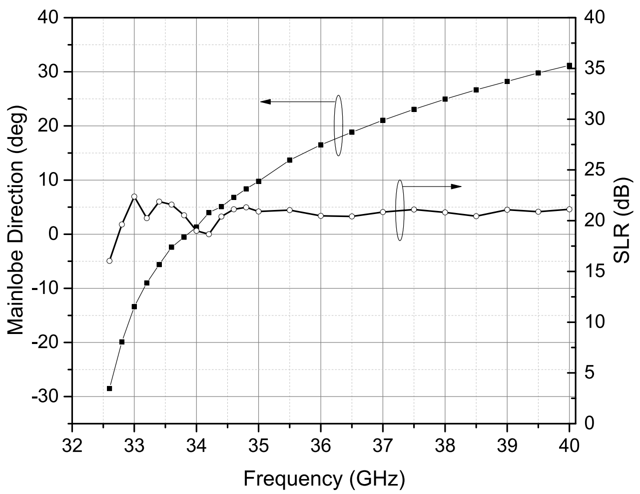

FIGURE 16. Mainlobe directions and SLRs of the meandering long slot CRLH waveguide LWA.

Fig. 17 shows the realized gain and radiation efficiency of this meandering long slot CRLH waveguide LWA. As can be seen, larger than 17 dBi gain is achieved at most frequencies and the maximum gain is about 19.6 dBi from the measured gain curve. A slight discrepancy between the simulated and measured gains is observed near 34 GHz, which is caused by the increased reflection loss because of the manufacture error. It is observed that the measured radiation efficiency is greater than 50% in the major operating band, and the maximum and the average efficiency is 77% and 65.4%, respectively.

Table 1 compares the SLLs between this work and other existing low SLL tapered LWAs. It is seen that most of the designs are able to achieve a relative low SLL at single frequency only. In [10], a CRLH ridge substrate integrated waveguide (RSIW) slot array was realized with −15 dB SLL achieved only in the LH region. Besides, the radiation efficiency is less than 50% in the operating band because

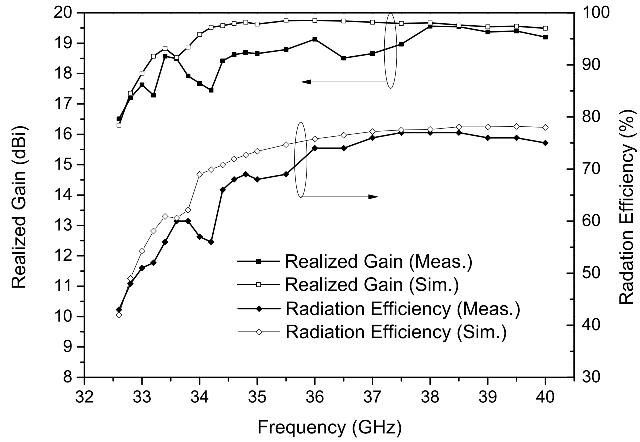

FIGURE 17. Realized gain and radiation efficiency of the meandering long slot CRLH waveguide LWA.

of the high dielectric loss. In [13], SLL below −15 dB was realized in a narrow beam-steering range from −3.6° to +7.6°, however, only simulated results were provided. Similar waveguide strucures were found in [19] and [26]. In [19], the CRLH waveguide slot array was synthesized using Elliott's classic slot array design procedure. Patterns at only 3 frequency points were given and at the same time, the dielectric corrugations of the CRLH waveguide led to high dielectric loss. The slot array in [26] used the same CRLH waveguide as our design, however, SLL of −22 dB was achieved at only single frequency of 8.5 GHz. A traditional microstrip periodic LWA with backward to forward scanning capability was reported in [27], the OSB has been suppressed by matching the input impedance of the unit cell to the characteristic impedance of the transmission line so that the broadside radiation is possible. However, only −12 dB SLL was realized by the tapered LWA with the scanning range from −14° to +16°. A low SLL traditional LWAs was proposed in [28]. Its beam-steering range is restricted in the forward quadrant. Besides, the low SLL patterns are only reported in a small beam-steering range, as shown in Table 1. In [29], a periodic collinear-slotted RSIW LWA with OSB elimination was reported. A good measured SLL performance of −20 dB was accomplished within the beam-steering range from −35° to +35°. However, the low power capacitance of this planar structure makes it unsuitable to the detective radar application. A microstrip LWA was proposed in [30] by periodically loading shunt radiation element pairs along a host transmission line. The measured SLL keeps almost −23 dB at around 0°, but a deviation occurs when the main lobe is steered away from broadside. In this work, SLL below −18.5 dB is realized from 32.8 GHz to 40 GHz with a wide beam-steering range from −20° to +31°. Compared with the other designs in Table 1, the SLL performance and the corresponding beam-steering range surpass most of the other designs. Another advantage of the proposed meandering long slot CRLH waveguide LWA

TABLE 1. SLL comparison with existing tapered LWAs.

Designs	Antenna Type	SLL (dB)
[10]	RSIW slot array	-15 within LH region
[11]	SIW	-16 @ $0°$
[12]	SIW	-13.3 @ $25°$
[13]	SIW sparse array	< -15 within $[-3.6°, 7.6°]$
[19]	waveguide slot array	-24 @ $-20°$; -17 @ $0°$ & $20°$
[26]	waveguide slot array	-22 @ $-11°$
[27]	microstrip	< -12 within $[-14°, +16°]$
[28]	SINRD waveguide	< -17.4 within $[-24.9°, -22°]$
[29]	RSIW	< -20 within $[-35°, +35°]$
[30]	microstrip	< -13 within $[-20°, +30°]$
This work	**waveguide LWA**	$< \mathbf{-18.5}$ **within** $[\mathbf{-20°}, \mathbf{+31°}]$

lies in the avoidance of grating lobes. As is known to all, the grating lobes in a beam-steering array will not appear when the element distance d_e satisfies

$$\frac{d_e}{\lambda} \leq \frac{n-1}{n(1+|\sin\theta_M|)} \tag{4}$$

where n is the element number, and θ_M is the maximum beam-steering direction. It would be very difficult to control the element distance if the antenna operates at or above Ka-band, while by using the continuous meandering long slot on the waveguide, this problem can be avoided.

V. CONCLUSION

A high performance CRLH waveguide LWA with low SLL and high radiation efficiency is designed, manufactured and measured in this paper. The analysis procedure is investigated intensively. A prototype of the CRLH waveguide LWA with meandering long slot is designed and fabricated. Measured results show that SLR above 18.5 dB is realized in the major operating band with a wide beam-steering range from $-29°$ to $+31°$, which is seldom seen in other existing CRLH LWA designs. The measured radiation efficiency larger than 50% is reached in the major operating band. The high performance of the designed CRLH LWA shows a potential application in practical radar systems.

ACKNOWLEDGMENT

The authors would like to thank Mr. X. Li and Dr. M. Yi (National Space Science Center, Chinese Academy of Sciences) for their kind help and advice in the antenna fabrication and measurement.

REFERENCES

[1] A. Oliner and D. Jackson, *Antenna Engineering Handbook Leaky-Wave Antennas*, 4th ed. J. L. Volakis, Ed. New York, NY, USA: McGraw-Hill, 2007.

[2] R. Hansen, *Microwave Scanning Antennas: Array systems*, vol. 3. New York, NY, USA: Academic, 1966.

[3] C. Caloz and T. Itoh, *Electromagnetic Metamaterials: Transmission Line Theory and Microwave Applications: The Engineering Approach*. Hoboken, NJ, USA: Wiley, 2006.

[4] L. Liu, C. Caloz, and T. Itoh, "Dominant mode leaky-wave antenna with backfire-to-endfire scanning capability," *Electron. Lett.*, vol. 38, no. 23, pp. 1414–1416, Nov. 2002, doi: 10.1049/el:20020977.

[5] C. Jin, A. Alphones, and L. C. Ong, "Broadband leaky-wave antenna based on composite right/left handed substrate integrated waveguide," *Electron. Lett.*, vol. 46, no. 24, pp. 1584–1585, Nov. 2010.

[6] Y. D. Dong and T. Itoh, "Composite right/left-handed substrate integrated waveguide and half mode substrate integrated waveguide leaky-wave structures," *IEEE Trans. Antennas Propag.*, vol. 59, no. 3, pp. 767–775, Mar. 2011.

[7] Y. D. Dong and T. Itoh, "Substrate integrated composite right-/left-handed leaky-wave structure for polarization-flexible antenna application," *IEEE Trans. Antennas Propag.*, vol. 60, no. 2, pp. 760–771, Feb. 2012.

[8] Q. Yang, Y. Zhang, and X. Zhang, "X-band composite right/left-handed leaky wave antenna with large beam scanning-range/bandwidth ratio," *Electron. Lett.*, vol. 48, no. 13, pp. 746–747, Jun. 2012.

[9] Q. Yang, X. Zhang, and Y. Zhang, "A shunt-capacitance-aided composite right/left-handed leaky wave antenna with large scanning-range/bandwidth ratio," in *Proc. PIERS*, 2012, pp. 649–652.

[10] Q. Yang, X. Zhao, and Y. Zhang, "Composite right/left-handed ridge substrate integrated waveguide slot array antennas," *IEEE Trans. Antennas Propag.*, vol. 62, no. 4, pp. 2311–2316, Apr. 2014.

[11] H. Lee, Y. Kasahara, and T. Itoh, "Study of high efficiency and low sidelobe level CRLH leaky-wave antenna based on short-end and tapered cells," in *Proc. 44th Eur. Microw. Conf.*, Oct. 2014, pp. 251–254.

[12] Q. Bai and J. Wang, "Composite right/left-handed substrate integrated waveguide leaky-wave antenna array with low sidelobe level and high gain," in *Proc. 7th IEEE Int. Symp. Microw. Antenna Propag. EMC Technol. (MAPE)*, Oct. 2017, pp. 37–40.

[13] L. Yang, H. Wang, X. Jiang, and Y. Huang, "Composite right/left-handed substrate integrated waveguide leaky-wave sparse array antenna with low sidelobe level," in *Proc. 46th Eur. Microw. Conf. (EuMC)*, Oct. 2016, pp. 1279–1282.

[14] J. Liu, W. Zhou, and Y. Long, "A simple technique for open-stopband suppression in periodic leaky-wave antennas using two nonidentical elements per unit cell," *IEEE Trans. Antennas Propag.*, vol. 66, no. 6, pp. 2741–2751, Jun. 2018.

[15] W. Zhou, J. Liu, and Y. Long, "Investigation of shorting vias for suppressing the open stopband in an SIW periodic leaky-wave structure," *IEEE Trans. Microw. Theory Techn.*, vol. 66, no. 6, pp. 2936–2945, Jun. 2018.

[16] Y. L. Lyu X.-X. Liu, P.-Y. Wang, D. Erni, Q. Wu, C. Wang, N.-Y. Kim, and F.-Y. Meng, "Leaky-wave antennas based on noncutoff substrate integrated waveguide supporting beam scanning from backward to forward," *IEEE Trans. Antennas Propag.*, vol. 64, no. 6, pp. 2155–2164, Jun. 2016.

[17] I. A. Eshrah, A. A. Kishk, A. B. Yakovlev, and A. W. Glisson, "Rectangular waveguide with dielectric-filled corrugations supporting backward waves," *IEEE Trans. Microw. Theory Techn.*, vol. 53, no. 11, pp. 3298–3304, Nov. 2005.

[18] M. Navarro-Tapia, J. Esteban, and C. Camacho-Peñalosa, "Initial assessment of a waveguide with dielectric-filled corrugations as a technology for slot antennas with backward-to-forward scanning capabilities," *Metamaterials*, vol. 3, no. 3, pp. 174–184, 2009.

[19] M. Navarro-Tapia, J. Esteban, and C. Camacho-Penalosa, "On the actual possibilities of applying the composite right/left-handed waveguide technology to slot array antennas," *IEEE Trans. Antennas Propag.*, vol. 60, no. 5, pp. 2183–2193, Mar. 2012.

[20] K. Dong-Jin and L. Jeong-Hae, "Beam scanning leaky-wave slot antenna using balanced CRLH waveguide operating above the cutoff frequency," *IEEE Trans. Antennas Propag.*, vol. 61, no. 5, pp. 2432–2440, May 2013.

[21] A. M. N. Eldeen and I. A. Eshrah, "CRLH waveguide with air-filled double-ridge corrugations," in *Proc. IEEE Int. Symp. Antennas Propag. (APSURSI)*, Jul. 2011, pp. 2965–2968.

[22] Q. Yang, X. Zhao, and Y. Zhang, "CRLH waveguide based ka-band beam-steering leaky-wave antenna for radar application," in *Proc. PIERS*, 2015, pp. 2820–2823.

[23] Q. Yang, X. Zhao, and Y. Zhang, "Leaky-wave radiation analysis for CRLH waveguide with long slot on its broadwall," in *Proc. 10th Eur. Conf. Antennas Propag. (EuCAP)*, Apr. 2016, pp. 1–5.

[24] Q. Yang, X. Zhao, and Y. Zhang, "High performance CRLH waveguide leaky-wave antenna with optimized sidelobe level," in *Proc. IEEE Int. Symp. Antennas Propag. & USNC/URSI Nat. Radio Sci. Meeting*, Jul. 2017, pp. 1175–1176.

[25] Q. Yang, X. Zhao, and Y. Zhang, "Electromagnetic analysis on propagation characteristics of crlh waveguide loaded with double ridge corrugations," *Prog. Electromagn. Res. C*, vol. 75, pp. 1–11, 2017.

[26] F. Siaka, J. J. Laurin, and R. Deban, "New broad angle frequency scanning antenna with narrow bandwidth based on a CRLH structure," *IET Microw. Antennas&Propag.*, vol. 11, no. 11, pp. 1644–1650, 2017.

[27] M. H. Rahmani and D. Deslandes, "Backward to forward scanning periodic leaky-wave antenna with wide scanning range," *IEEE Trans. Antennas Propag.*, vol. 65, no. 7, pp. 3326–3335, Jul. 2017.

[28] P. F. Kou and Y. J. Cheng, "Ka-band low-sidelobe-level slot array leaky-wave antenna based on substrate integrated nonradiative dielectric waveguide," *IEEE Antennas Wireless Propag. Lett.*, vol. 16, pp. 3075–3078, 2017.

[29] A. Mallahzadeh and S. Mohammad-Ali-Nezhad, "Periodic collinear-slotted leaky wave antenna with open stopband elimination," *IEEE Trans. Antennas Propag.*, vol. 63, no. 12, pp. 5512–5521, Dec. 2015.

[30] Y.-L. Lyu, F.-Y. Meng, G.-H. Yang, P.-Y. Wang, Q. Wu, and K. Wu, "Periodic leaky-wave antenna based on complementary pair of radiation elements," *IEEE Trans. Antennas Propag.*, vol. 66, no. 9, pp. 4503–4515, Sep. 2018.

QINGSHAN YANG (S'12–M'14) was born in Anhui, China, in 1987. He received the B.S. degree in electrical engineering from Xidian University, Xi'an, China, in 2008, and the Ph.D. degree in electrical engineering from the University of Chinese Academy of Sciences (UCAS), Beijing, China, in 2014.

From 2014 to 2017, he was an Assistant Professor with the National Space Science Center, Chinese Academy of Sciences (CAS), Beijing. He is currently an Associate Professor with the National Space Science Center, CAS. He has been a member of the Youth Innovation Promotion Association of CAS, since 2017. His research interests include the microwave circuits, antenna arrays, metamaterials, and radar systems.

XIAOWEN ZHAO (S'15–M'16) was born in Shaanxi, China, in 1987. She received the B.S. degree in electrical engineering from Xidian University, Xi'an, China, in 2011, and the Ph.D. degree in electrical engineering from the University of Chinese Academy of Sciences (UCAS), Beijing, China, in 2016.

Since 2016, she has been an Assistant Professor with the National Space Science Center, Chinese Academy of Sciences (CAS), Beijing. Her research interests include the antennas, array synthesis, and compressed sensing.

Dr. Zhao was a recipient of the CAS Presidential Scholarship, in 2016 and the Outstanding Graduates Award of Beijing, in 2016.

YUNHUA ZHANG (M'00) was born in Hunan, China, in 1967. He received the B.S. degree in electrical engineering from Xidian University, Xi'an, China, in 1989, and the M.S. and Ph.D. degrees in electrical engineering from Zhejiang University, Hangzhou, China, in 1993 and 1995, respectively.

He is currently a Professor with the National Space Science Center, Chinese Academy of Sciences, the Deputy Director of the Key Laboratory of Microwave Remote Sensing, Chinese Academy of Sciences. He has published more than 100 SCI/EI articles in domestic/international journals, and in international conference proceedings. His research interests include the system design and signal processing of microwave sensors (high-resolution radar, interferometric radar, radar altimeter, and noise radar), polarimetric radar target decomposition, application of compressive sensing in radar, and antennas and computational electromagnetics.